Cable Modem architectures adapted to the noise problem in the upstream direction for multiple access Hybrid Fiber Coax Networks

Johan Haspeslagh[a], Geert Goris[a], Mark Van Bladel[b], Heidi Steendam[b], Teresa Marongiu[b], Marc Moeneclaey[b], Elke Claus[c], Jon Vandenbruaene[c], Luc Martens[c], Paul Gabriel[d]

[a]Alcatel Alsthom – Corporate Research Center Antwerp, Belgium

[b]University of Ghent, Communication Engineering Lab, Ghent, Belgium

[c]Imec–Intec, Ghent, Belgium

[d]Barco, Kortrijk, Belgium

ABSTRACT

As interactive services require more bandwidth, high speed access networks must follow this trend. Although a Hybrid Fiber Coax (HFC) system provides a large bandwidth, many problems occur due to the accumulation of the ingress and impulse noise. In this paper the properties of the ingress and impulse noise will be explained based on a measurement campaign on different networks.

The most striking result of the measurement campaign is the large dynamic and time–dependent behavior of the ingress noise. This dynamic behavior is an important factor in designing an upstream communication system. We show that for this reason optimized receivers will contain adaptive equalizers. This is illustrated by the performance analysis of a TDMA and an OFDM–CDMA system. Both systems are compared under the same environment. The results of this comparison shows how both can obtain the same performance.

Considering the implications of both the TDMA and the CDMA system when using an equalizer in the head–end receiver, requirements for a total HFC network architecture are given. Especially synchronization and initialization issues must be addressed.

1. INTRODUCTION

As services available on the internet, videoconference, home working ... require more bandwidth and are getting more popular, high speed access networks must follow this trend. The hybrid fiber coax network can be and will be one of the major players in that field. Coax networks historically make large bandwidths available in the downstream direction. In the lower frequency band designated for the upstream direction however, severe ingress and impulse noise can be observed.

In a first part the network architecture in the upstream direction and the considered bandwidth usage will be explained.

In a second part an overview of measurements performed on a live network will be presented. The measurement method has been conceived in such way that it presents relevant parameters in the design of a communication system.

It will be shown that ingress noise is a severe problem for frequencies under 20 MHz and that impulse noise is dominant under 10 MHz. Also the dynamic behavior of ingress noise will be emphasized.

Using the outcome of these measurements, different possible multiple access and modulation techniques will be analyzed in a third part. Since the hybrid fiber coax network is a bandwidth and power limited environment, general conclusions on performance bounds for several approaches in modulation and access can be given. Particular attention will be paid to the use of adaptive filtering for CDMA–multitone and TDMA–QAM transmission techniques.

Part of the EUROPTO Symposium on Broadband European Networks
Zurich, Switzerland • May 1998 • SPIE Vol. 3408 • 0277-786X/98/$10.00

Finally the implementation issues of the introduction of an adaptive equalized receiver in a HFC network are considered. The aspects concerning multiple access and the provisioning of the system are addressed.

2. NETWORK ARCHITECTURE

The general concept of an HFC network is shown in Figure 1 An access node in the backbone network is connected to an access–adapter, called headend. This access adapter contains the line termination (LT) to the HFC side. It also performs the electrical/optical conversion at the network side. The coax network is also connected through an optical/electrical converter. The coax network is terminated at the premises by the HFC NT. In downstream direction broadcasting is performed from the head–end to all HFC–NT's. In the upstream direction an access mechanism must be provided.

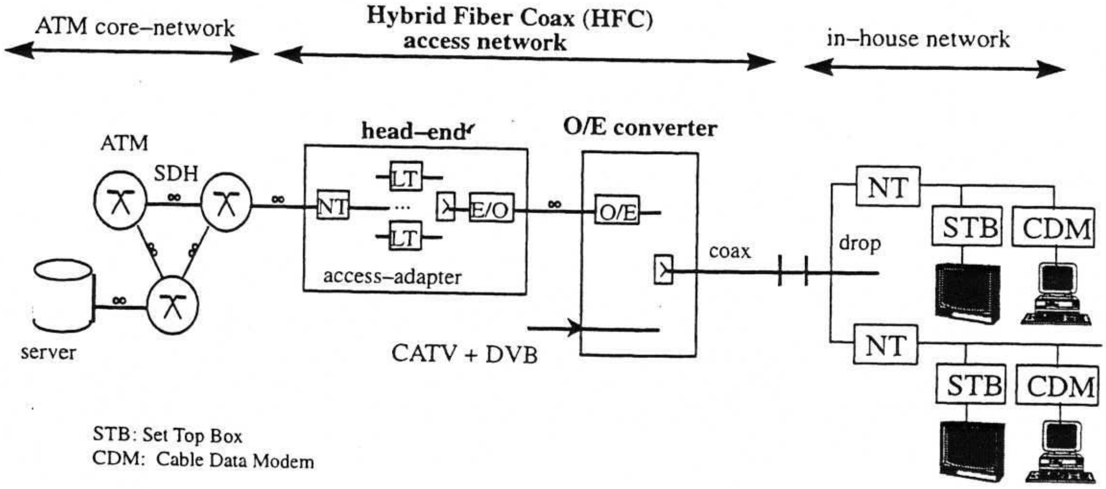

Figure 1 :Network architecture

A typical coax access network may contain a few 100 to 1000 homes passed, depending on the service penetration.

In order to provide interactive digital services on the existing coax network specific frequency slots must be allocated. The downstream range starts from 50 and 80 MHz and extends up to 400 MHz–1 GHz depending on the performance of the network elements. The upstream spectrum starts from about 5 MHz and ends at 30–50 MHz. Upstream–downstream separation is realized by using duplex splitting filters in each distribution and trunk amplifier of the coax–network.

3. UPSTREAM NETWORK CHARACTERIZATION

As the upstream channel is a shared access channel, noise from each subscriber is collected and is funneling through the network to the head–end [1] [2] [3]. It is estimated that 70% of the noise in the head–end originates from the subscriber's home and 25% in the coaxial drop. Two types of noise are present: ingress and impulse noise. Ingress noise are narrow–band signals that are relatively slowly varying while impulse noise is composed of bursts or spikes in time with large spectral contents [3] [4]. Measurements of ingress and impulse noise have been performed on 2 different networks containing about a 600 and 1300 subscribers respectively. The first network has mainly buried cable and serves a residential area close to harbor activities. The second network is a mixture of buried and wall–mounted cable serving a more or less residential area incorporating high buildings.

3.1. Ingress measurements

Ingress noise can be modeled as a combination of a frequency dependent background noise (produced by for examples the amplifiers) and high peaks of noise concentrated in small frequency bands (produced by short–wave broadcast or CB transmitters for example) [4] [5].

We have made the following observations:

- The buried network has a slightly lower background noise, but peak ingress has the same level.
- Radio background noise is dominant at the lower frequencies up to 20 MHz.
- High peaks tend to be concentrated in broadcast bands.
- Ingress noise fluctuations of 20 dB or more are observed in a time span of a few seconds.

Peak variations are concentrated (but not exclusively) around certain bands (mostly broadcast bands). There is also a clear day–night variation. Above 18–20 MHz such high variations occur less frequently.

The allocation of frequency bands without severe ingress impact is very difficult. Figure 2 shows the peak variations of the ingress noise in bandwidths of 2 MHz. Variations between 5 and 30 dB can occur. For the band around 27 MHz the variation is even in the order of 40 dB.

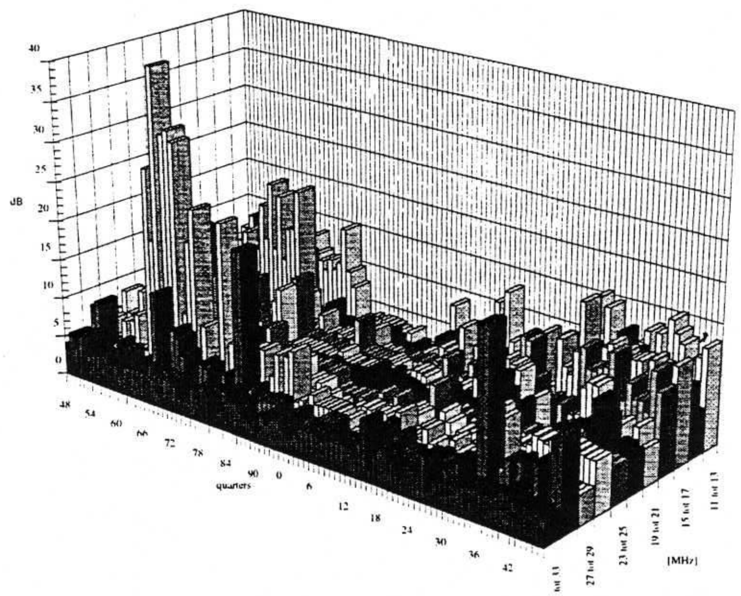

Figure 2 :Peak dynamic behavior in 2 MHz bins

In Figure 3 , the time duration of the ingress noise peaks is illustrated. A distribution is given showing the number of bursts occurring with a certain length per frequency band. A length of 1 corresponds to approximately 1 second. Each frequency band considered has a width of 30 kHz. A burst is considered to have an amplitude > –20 dBmV/$\sqrt{\text{Hz}}$. It is observed that background noise levels may be in the order of –50 to –70 dBmV/$\sqrt{\text{Hz}}$.

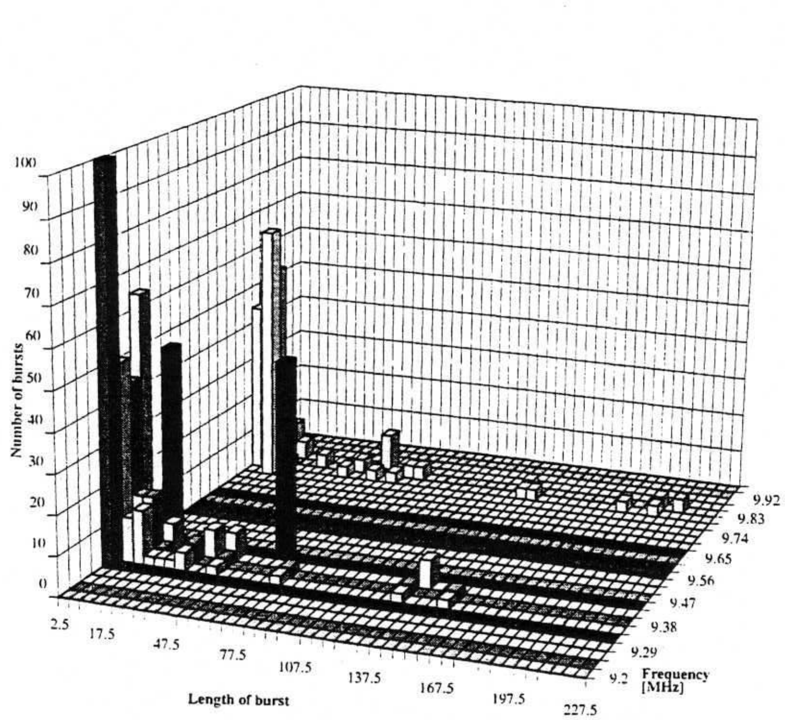

Figure 3 : Burst noise distribution versus length of burst

3.2. Impulse noise measurements

Impulse noise is mainly due to impulsive emissions from electrical motors and switches. It is important to consider the impulse energy and envelope waveform in the frequency band of interests, meaning the upstream channel frequency band. Most of the energy of the impulse bursts is concentrated below 10 MHz.

The impulse noise was recorded with an oscilloscope in sequential mode during 24 hours. The maximum measurable trace was 327 µs long. In one trace, two spikes or bursts were considered as two pulses if they were separated minimally 5 µs. Since the impulse noise appears as spikes above the ingress noise, the threshold level was set to 6 dB above the ingress noise. Since the results of both networks are very similar, only the measurements on the network with 1300 subscribers are presented.

A total number of 131830 pulses has been recorded. The measured pulses were filtered in several 4 MHz channels for the band of 5–50 MHz. The threshold level to determine whether a pulse occurs was the same for all bands and equal to the measurement threshold level. For each channel the pulses are divided in several pulse width classes, amplitude classes and inter–arrival time classes. In this way we obtain the pulse width distribution, the amplitude distribution, and the distribution of inter–arrival times between pulses of the same pulse width class.

Figure 4 shows that the percentage of pulses remaining after filtering decreases with increasing frequency (100% is the number of pulses in the 5–50 MHz band). This means that the energy of the impulse bursts is concentrated in the lower bands.

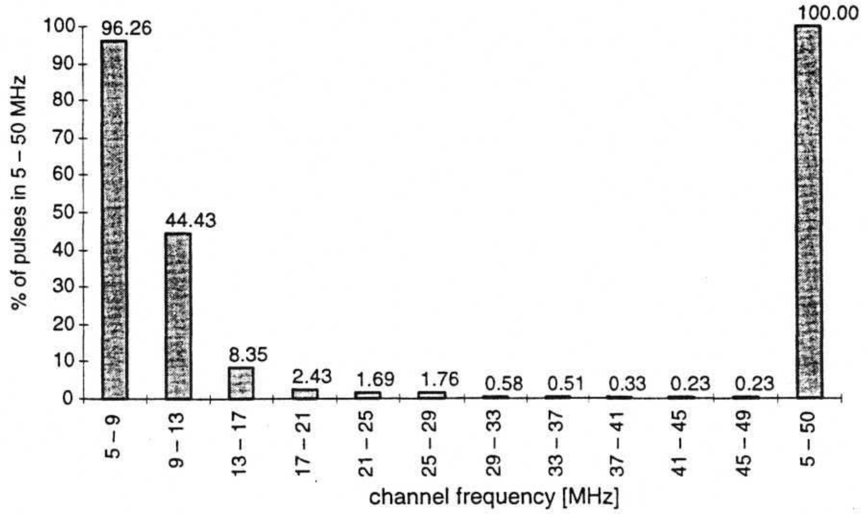

***Figure 4** :Percentage of pulses in upstream frequency bands.*

The pulse width distribution in each frequency band learns us that 95% of the pulses in each frequency band is shorter than 50 µs. We also found that the pulse width decreases with increasing frequency. Figure 5 for example shows the pulse width distribution in the 13 to 17 MHz band. The majority of the pulses is even shorter than 5 µs.

The inter–arrival times (= time spacing between pulses) within a pulse width class increase with increasing frequency. So the higher the frequency, the longer it takes to detect a new pulse in the same pulse width class. A more detailed look at the results learns us that about 50 % of the pulses with inter–arrival times between 0 and 50 µs are in the 5–10 and 10–15 µs inter–arrival time classes. The inter–arrival time is also an ascending function of the pulse width: the longer the pulses, the longer the inter–arrival times in between them. When we compare in Figure 6 (a) with (b) we can clearly see that the inter–arrival times for pulse widths between 15 and 20 µs are mostly in the seconds range while they are in the microseconds range for pulse widths between 0 and 1 µs.

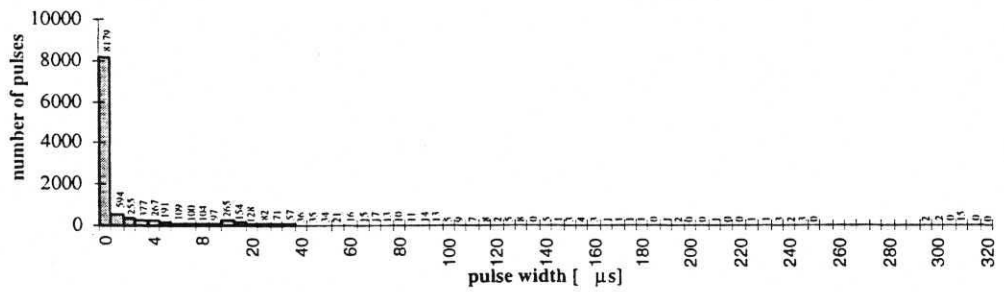

***Figure 5** :Pulse width distribution in the band 13–17 MHz.*

We can conclude that the inter–arrival times for the short pulses originate mainly from pulses in the same trace, while the inter–arrival times between longer pulses originate from pulses in different traces.

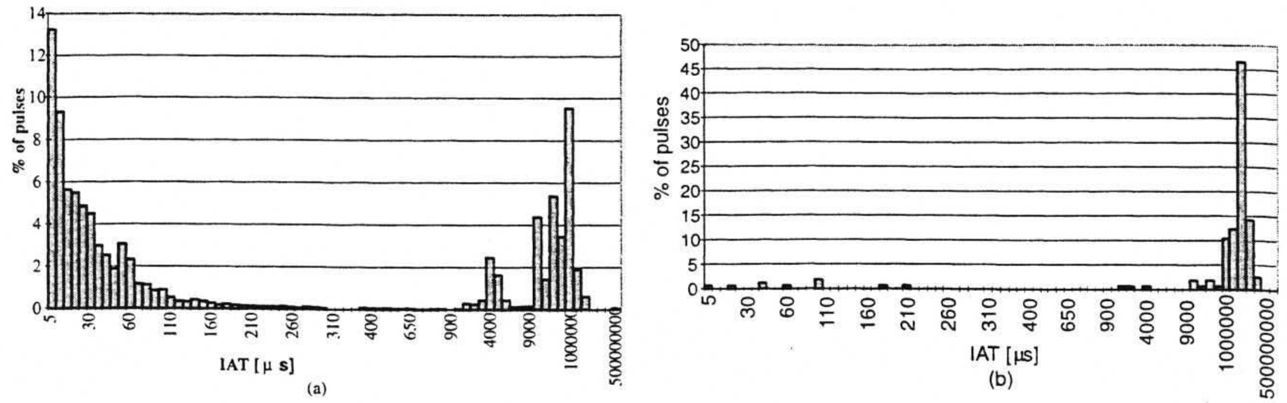

Figure 6 :Inter–arrival times in band 13–17 MHz for pulse widths, (a) between 0 and 1 μs and (b) between 15 and 20 μs.

Figure 7 shows an example of the amplitude distribution. The amplitude is defined as the maximum value the pulse reaches during an impulse burst period. Approximately 90% of the pulses have an amplitude between the threshold level and five times this level. The absolute number of pulses with an amplitude of at least five times the threshold level is a descending function of the frequency. However, in the network with 600 subscribers the amplitude decrease was more pronounced than in the network with 1300 subscribers.

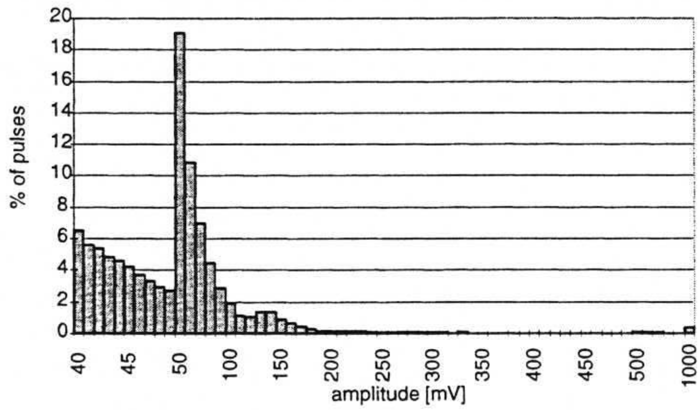

Figure 7 :Amplitude distribution in the band 13–17 MHz.

4. Possible modulation and access techniques in upstream

4.1. General considerations

The coax part of a HFC network is a bandwidth and power limited environment. The fact that bandwidth and power has to be shared by all subscribers makes it quite different from a wireless network where the power limitation is given by the mobile unit.

As the measurement campaign showed that the most noticeable impairment is the ingress noise and its dynamic behaviour, the Matched Filter Bound (MFB) has been used to define an upperbound to the performance. The Matched Filter Bound is defined as the best signal to noise ratio obtained at an optimum receiver when sampled optimally for a one term sequence.

In a non–white and non–stationary noise environment an instanteneous MFB could be defined, which can practically only be approximated by introducing adaptation in the system. Each access method (TDMA, FDMA, CDMA) can be modified to incorporate adaptation.

Adaptation methods can be roughly divided in 2 types.

- A first one, the multicarrier approach, divides the usable bandwidth in small bins and optimizes the bitrate for each bin individually.
- A second one, the single carrier approach, takes the largest possible bandwidth and uses adaptive filtering.

The first approach is used in ADSL and is called there discrete multitone (DMT). The latter method is used in most standards for HFC downstream (IEEE802.14, DVB, MCNS standards).

Adaptation with DMT modulation is introduced by changing the constellation sizes per DMT tone. This operation must be performed via messages in the transmission convergence layer and supposes synchronization. This operation is not instantaneous. In a fast dynamic environment data may be lost over a long period during this adaptation. Therefore this method is better suited for stable or slow varying environments (like the twisted pair), where this form of adaptation is rather an exception than a rule.

For a fast varying environment local adaptation at the head–end receiver is to be preferred. One way to achieve this is to use an adaptive equalizer in conjunction with TDMA or CDMA.

It is noted that FDMA or OFDMA is more difficult to use with adaptive filtering as they tend to converge to the DMT solution for small frequency channel spacings. Methods better suited to use with (O)FDMA are hopping techniques with error correction/interleaving. OFDM schemes will not be considered here.

4.2. TDMA approach

As a test vehicle we consider the baseband equivalent model of a transmitter receiver chain shown in Figure 8 .

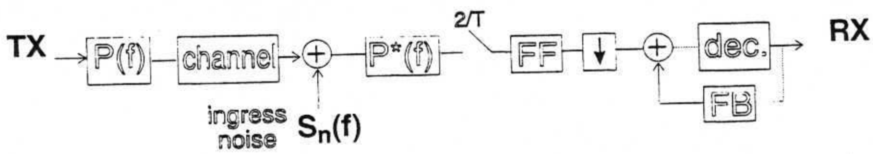

Figure 8 :Equivalent baseband model of the head–end receiver

The transmitter is modelled by its pulse–shaping filter P(f), which is typically a square root raised cosine filter. The channel models the amplitude and group delay. Sn(f) represents the ingress noise power spectrum. The ingress noise is modelled as additive coloured Gaussian noise. The receiver contains first a filter matched to the pulse–shaping filter P(f) in the transmitter. This matched filter is followed by a fractionally–spaced decision feedback equalizer. The signal is sampled at twice the baudrate (1/T).

This scheme was found to give better results than that with a receiver filter matched to the received pulse, i.e. $P^*(f).Hch^*(f)/\sqrt{Sn(f)}$, yields the theoretical optimal signal–to–ingress noise ratio, but introduces an enormous amount of intersymbol interference(ISI). Structures which can easily compensate for ISI are thus preferrable.

Analysis based on some worst case ingress noise spectra has shown that in order to obtain a performance close to the limit of an infinite length equalizer, the forward equalizer FF must have between 10 and 50 taps and the feedback equalizer FB somewhere between 10 and 100 taps. It is noted that such an equalizer determines the hardware complexity in the receiver.

The following system will be considered.

System proposal for the TDMA system	
baudrate	6.95 Mbaud
roll–off factor	0.15
channel spacing	8 MHz
central frequency	12 MHz
Forward equalizer taps	25
Feedback equalizer taps	50
signal constellation (for analysis)	QPSK
Number of users at a mean 64 kbit/sec rate	256

The 8 MHz channel corresponds with present state of the art modem integration technology which will be used in e.g. VDSL.

As performance criterion, the signal to noise ratio at the slicer is taken. Because this value can directly be transformed to a BER for a particular constellation, it is generic. The performance analysis has been done in the following way.

- 15 minutes of ingress noise traces (5–60 MHz) have been selected from our database.
- For each trace the signal to noise ratio at the slicer of the receiver has been calculated.
- The power of the transmitter has then been chosen in order to obtain only 1 trace with a BER as high as 10^{-3} when using QPSK modulation with a receiver containing an adaptive equalizer.

The ingress noise traces were collected at the head–end of a site with approximately 1000 subscribers. The required signal power–spectral–density was found to be Es = –91 dBm/Hz.

Figure 9 gives the signal to noise ratio for a non–equalized and Figure 10 for the equalized system for the same transmit power. Note that for the transmission of uncoded QPSK over an AWGN channel with a BER of 10^{-3} a SNR of at least 9.8 dB is required. A bit error rate of 10^{-3} corresponds to a BER of 10^{-8} after channel coding.

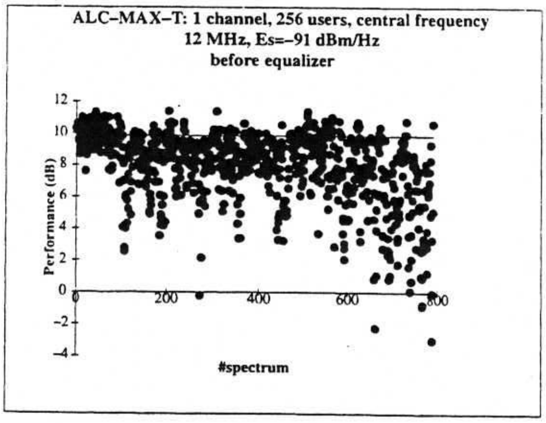

Figure 9 :Signal to noise ratio of the non–equalized receiver

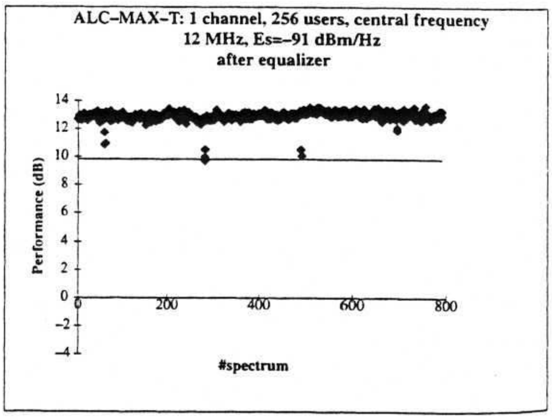

Figure 10 :Signal to noise ratio of the equalized receiver

The non–equalized system shows that if present day available commercial modems would use this wide bandwidth and this power they presumably would fail. The results of the non equalized system show also large fluctuations in performance for an non–equalized system. In order to obtain the required performance, the transmission power should at least be 12 dB higher.

The equalized system has a gain of approximately 2 dB when comparing the best traces between the equalized and non–equalized system. But of more importance, fluctuations in performance are reduced to a few dB. Thus an equalized system is beneficial with regard to power requirements and robustness.

These results are based on static noise calculations. A real world system must be able to track the noise variation. Performance under tracking conditions are dependent not only on the equalizer architecture but also on the update algorithm. Simulations were done using a least–mean–square (LMS) algorithm both in time and in frequency domain. Frequency domain equalization is known to offer better convergence speed properties. However, simulations showed for this application no substantial gain could be obtained from a frequency domain approach.

4.3. The OFDM–CDMA approach

As CDMA is based on spread spectrum modulation it is also a wide bandwidth approach. CDMA used for wireless applications, allows only non–synchronized operation. In HFC however using asynchronous CDMA would only reach 20% of the capacity of other access schemes. Therefore synchronization up to chip level is necessary. It must be accurate in the order of 1/8 –1/16 of the chiplength for low performance loss. It should be noted that this synchronization has to be controlled via ranging mechanisms in the downstream path and is thus critical.

By combining OFDM and CDMA one can profit from the longer symbol length while keeping the wide spreading bandwidth. The longer symbol length of OFDM allows the introduction of a guard band, which diminishes the user–dependency in the network optimization.

There are different methods described in the literature [6],[7] to combine OFDM with CDMA. What is proposed here is similar to ref. [8],[9]. Each tone of the OFDM spectrum is attributed to one chip of the spreading code. A transmit symbol is presented to all tones and is multiplied by its associated chip. A symbol of a subscriber is thus transmitted over the period of one OFDM symbol as is shown in Figure 11

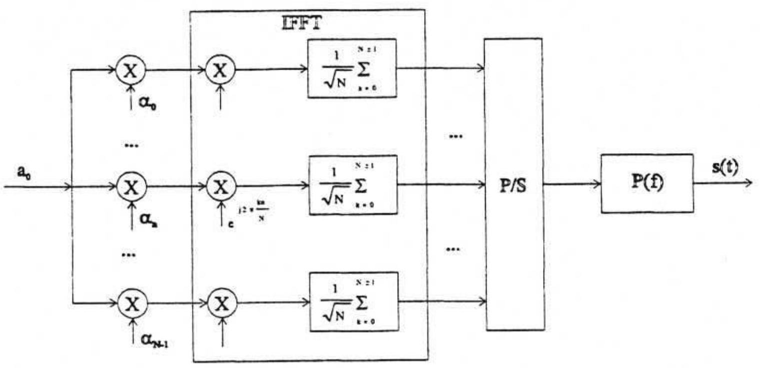

Figure 11 :OFDM–CDMA transmitter baseband equivalent structure

The receive signal contains the contributions of all subscribers. First an FFT is performed on the incoming signal. Each tone contains the sum of all subscriber symbols for the chip associated with that tone. To obtain the symbol of a specific subscriber the output of the FFT is correlated with the appropriated code sequence.

It is clear that when ingress noise is present some tones at the FFT will be more affected than others. To avoid the performance loss caused by the highly affected tones, the receiver can be optimized by introducing a weighting filter as shown in Figure 12 , which is implemented adaptive to meet the variance in time of the ingress noise. When minimizing the performance loss caused by this ingress however, this filter strongly affects the orthogonality between the different CDMA codes and engenders a huge amount of multiple code interference, which will obstruct reliable communication. Considering both ingress and multiple code interference, a set of optimal filter coefficients, minimizing the total performance loss caused by both noise contributions, can be found using a LMS algorithm.

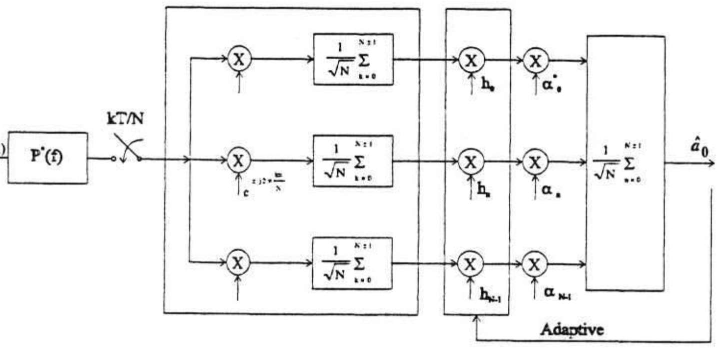

Figure 12 :OFDM–CDMA Receiver baseband equivalent structure

To perform an identical analysis as for the TDMA system, an OFDM–CDMA receiver with following specifications has been simulated. With the given channel transfer function a guard band as short as 8 samples proved to be sufficient.

System proposal for the OFDM–CDMA system	
baudrate	27 kbaud
roll–off factor	0.15
channel spacing	8 MHz
central frequency	12 MHz
number of tones	256
guard band	8 samples
signal constellation (for analysis)	QPSK
possible number of users at a mean 64 kbit/sec rate	256

Figure 13 gives the mean signal to noise ratio expected for each user. The SNR for a bit error rate of at least 10^{-3} is shown also.

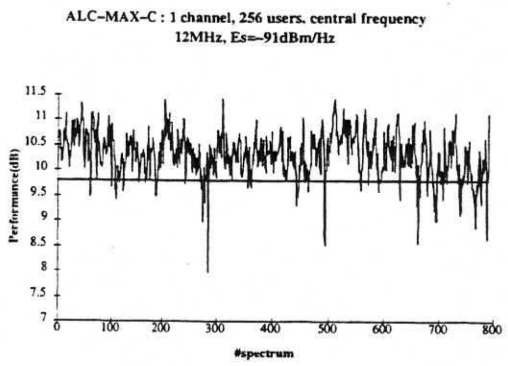

Figure 13 :Signal to noise ratio of the OFDM–CDMA system

Compared to the equalized TDMA scheme (Figure 10) it is noticed that there is an overall penalty of about 2 to 4 dB. The reason for this is two–fold:

- The FFT changes the noise spectrum seen by the decorrelator
- The weighting filter destroys the orthogonality between the codes.

For the first reason, the adaptive equalizer does not optimize on the basis of network noise spectrum, but on a transformed spectrum.

It is the second reason which determines for a large part the performance loss compared with the TDMA structure. An additional performance improvement can only be achieved by reducing the multiple code interference. In Figure 12 , a feedback section can be entered in the structure to eliminate the multiple code interference. Assuming perfect decisions, the signal after elimination of the multiple code interference is still disturbed by the ingress noise and requires an additional filter to diminish the effect of the ingress. This joint detection scheme will show a major performance improvement for channels severely affected by the ingress noise, as it can compensate for the performance loss caused by the ingress noise without introducing the high amount of multiple code interference. In some cases the performance of this structure will even exceed the performance of the TDMA structure with equalizer [10]. However, for channels who are not severely affected by highly peaked ingress noise, only a marginal gain in performance will be obtained notwithstanding the increased complexity of the structure. In this case, the performance is comparable to the performance of the TDMA structure with equalizer, even before elimination of the multiple code interference.

5. SYSTEM ARCHITECTURE

Introducing an adaptive equalizer in a multiple access system imposes some requirements on the architecture of the network system.

The equalization in the proposed TDMA or OFDM–CDMA receiver must not be disturbed by the bursty traffic behavior of the subscribers. Timing and carrier frequency recovery must also be addressed. Following aspects have to be considered:

- Timing and carrier frequency differences between users may not interfere with the equalizer;
- Idle periods (no access on the channel) may not disturb the equalizer settings and its tracking behavior;
- Amplitude and phase characteristic differences between subscribers are to be compensated;

6. CONCLUSIONS

Ingress noise, especially when strongly varying in time, has been shown to be the limiting performance factor in the upstream direction of a HFC system, and thus determines the choice of a modulation–access scheme. It is shown that adaptive receiver schemes can cope with this phenomena.

Two schemes have been analyzed : a TDMA and an OFDM–CDMA based system.

Through analysis and simulations following conclusions were drawn.

1. Equalized systems may perform between 2 and 10 dB better than non–equalized systems using the same bandwidth.
2. Equalized systems are more robust in the varying noise environment.
3. The presented TDMA scheme performs slightly better than an OFDM–CDMA system without multi–user–interference cancellation.

7. ACKNOWLEDGEMENTS

The work reported has been carried out in the Hybrid Fiber Coax Systems Project (IT–HFCS) of the Flemish action program for Information Technology. The authors would like to thank the Flemish Authorities for the support obtained in these projects.

8. REFERENCES

1 C. A. Eldering, N. Himayat and F. M. Gardner, "CATV Return Path Characterisation for Reliable Communications", IEEE Commun. Mag., Vol. 33, No. 8, , pp. 62–69, Aug. 1995

2 R.P.C. Wolters, "Characteristics of Upstream Channel Noise in CATV networks", IEEE Transactions on Broadcasting, Vol. 42, No. 8, pp. 328–332, Dec. 1996

3 L.F. Lind and N.A. Mufti, "Efficient method for modeling impulse noise in a communication system", Electronics Letters, Vol. 32, No. 16, pp. 1440–1441, Aug. 1996

4 M. D. Carangi, W. Y. Chen, K. Kerpez and C. F. Valenti, "Coaxial Cable Distribution Plant Performance Simulation", SPIE, Vol. 2609, pp. 215–226, Jul. 1995

5 Cable Television Labs, "Two–Way Cable Television System Characterisation", 1995

6 K. Fazel, G. P. Fettweis, "Multi–Carrier Spread–Spectrum", Proc. of 1st workshop on Multi–Carrier Spread–Spectrum, April 1997, Oberpfaffenhofen, Germany, Kluwer Press

7 S. Hara, R. Prasad, "Overview of Multicarrier CDMA", IEEE Comm. Mag., Vol. 35, No.12, December 1997, pp. 126–133

8 V. M. DaSilva, E. S. Sousa, "Multicarrier Orthogonal CDMA Signals for Quasi–Synchronous Communication Systems", IEEE J. on Sel. Areas in Comm., Vol. 12, No. 5, June 1994, pp. 842–852

9 E. A. Sourour, M. Nakagawa, "Performance of Orthogonal Multicarrier CDMA in a Multipath Fading Channel", IEEE Trans. on Comm., Vol. 44, No. 3, March 1996, pp. 356–367

10 M. Van Bladel, H. Steendam, T. Marongiu, M. Moeneclaey, "Some TDMA and OFDM/CDMA Receiver Structures for Communication over the Return Path of the CATV Channel", to be presented at ICC '98, June 1998, Atlanta, GA (USA)